*SIMULATION OF SEMICONDUCTOR DEVICES AND PROCESSES Vol. 3*
*Edited by G. Baccarani, M. Rudan - Bologna (Italy) September 26-28, 1988 - Tecnoprint*

# NUMERICAL TREATMENT OF NONRECTANGULAR FIELD-OXIDE FOR 3D MOSFET SIMULATION

M. Thurner,P. Lindorfer, S. Selberherr

Institut für Allgemeine Elektrotechnik und Elektronik
Technische Universität Wien
Gusshausstraße 27–29, A–1040 Wien, AUSTRIA

*Abstract* – This paper presents results of a new numerical treatment of 3D MOSFET simulation with nonplanar interfaces. The simulations have been carried out by MINIMOS 5 our fully three–dimensional simulation program. Three–dimensional effects like threshold shift for small channel devices, channel narrowing and the enhanced conductivity at the channel edge have been successfully modeled.

## 1 Introduction

The shrinking dimensions of the elements of IC's require suitable device models in physics and mathematics for accurate simulation. The usual two–dimensional device simulations describe fairly well the electrical characteristics for wide channel transistors but the advanced VLSI technology led to serious problems in modeling very narrow channel devices and therefore a great demand appeared for 3D simulations. The three–dimensional effects in MOSFET's like the shift of the threshold voltage, enhanced conductivity or the large depletion region near drain at the channel edge caused by the finite channel width are not taken into account by the two–dimensional simulations [1]; the 2D programs are meanwhile state of the art. Accurate MOSFET device simulation requires suitable physical models but also skilled mathematical methods. Three–dimensional device simulation unfortunately needs a large amount of CPU–time and memory. It is therefore obviously necessary to incorpo-

rate very efficient algorithms. Demands on computer resources are usually kept moderate using rectangular shapes in simulation volume and planar interfaces.

In Chapter 2 we shall report about the physics and the mathematics on which the simulations of nonplanar interfaces are based. In addition we shall present the device structure and a consideration of some aspects of the oxide body of the MOSFET.

The results of our simulations carried out by MINIMOS 5 are reported in Chapter 3 and will be discussed there, too.

## 2 Physical and Mathematical Aspects

The basic equations which are implemented in our MINIMOS to describe current flow in silicon differ only slightly from the conventional equations. The Poisson equation and the continuity equations for electrons and holes are 'the' established basic equations which are commonly in use. A derivation of these equations can be found in e.g. [7]. The current relations for electrons and holes are somehow different from the conventional drift–diffusion relations. They include the hot electron transport effect. Detailed information on the 'hot–electron–transport' model can be found in [6,9]. In addition to the well known boundary conditions for the Poisson equation and the continuity equations we have to implement a boundary condition for the mobilities. We set the driving force $F$ as in (1).

$$\vec{F}_n|_{int} = 0 \tag{1}$$

If we neglect this boundary condition we get unrealistic mobilities near the interfaces. For solving the set of differential equations we apply for discretisation the box integration method after Forsythe [10] to deal with the boundary conditions of the nonrectangular interfaces. Integrating (2a) for discretisation at the interfaces we obtain the interface boundary condition (2b) implicitly.

$$\mathrm{div}(\ \varepsilon \cdot \mathrm{grad}\psi\ ) = \rho \tag{2a}$$

$$\varepsilon_{sem} \cdot \frac{\partial \psi}{\partial \vec{\vec{n}}}|_{sem} - \varepsilon_{ins} \cdot \frac{\partial \psi}{\partial \vec{\vec{n}}}|_{ins} = \sigma_{int} \tag{2b}$$

(2b) is the well known boundary condition at the semiconductor oxide interface which can be derived from (2a) by the law of Gauß. A detailed information about that special discretisation method can be found in e.g. [7],[10]. Using this method we split the integration volume around the grid point into the regions: semiconductor, oxide and contact. Every part of the integration volume will be provided with its respective material constant. At the semiconductor–oxide interface we can write the Poisson equation in normalized form for the point $x_i, y_j, z_k$:

$$\begin{aligned} A \cdot \psi_{i+1,j,k} + B \cdot \psi_{i-1,j,k} + C \cdot \psi_{i,j+1,k} + D \cdot \psi_{i,j-1,k} + \\ E \cdot \psi_{i,j,k+1} + F \cdot \psi_{i,j,k-1} + G \cdot \psi_{i,j,k} = \rho_{i,j,k} \cdot V_{sem} + \sigma_{i,j,k} \cdot A_{int} \end{aligned} \tag{3}$$

wherein $A = A_{sem} \cdot \varepsilon_{sem} + A_{ins} \cdot \varepsilon_{ins}$ and with analogous expressions for the coefficients $B, C, D, E, F, G$, $V_{sem}$ is the respective semiconductor volume, $\sigma$ is the interface charge and $A_{int}$ the interface area. A similar expression can be found for the current relations, neglecting the part of the integration volume which is situated in the oxide body. The geometry of the 3D MOSFET model is given in Fig. 1. We implemented an approximation to the complete oxide–volume which can be seen in Fig. 2. The upper plane denotes the interface of the oxide to the contacts and the surrounding volume, respectively. The lower plane denotes the interface of oxide and semiconductor. The definition of the interface is quite general and can be varied in a wide range. The gate contact is filled in the middle of the upper plane, the Source and Drain contacts are on the left and right. In the middle in the gate region the distance of the upper and lower plane equals the gate–oxide thickness. The drain currents calculated by 2D and 3D simulations cannot be compared in a straight forward manner if the field oxide is nonplanar. The oxide reduces gradually the channel width which is given by the mask specifications. Therefore we introduce an effective channel width $w_{eff}$ for the 2D current calculation instead of the given mask width. The effective channel width is calculated by (4)

$$w_{eff} = w - \frac{1.}{D_{ch}} \int_0^w fox(z)|_{l/2}\, dz \tag{4}$$

$w$ is the width specified by the mask, $D_{ch}$ denotes the channel depth, $l/2$ denotes half of the channel length, $fox(z)$ is the function which describes

the geometric of the channel in width direction.

## 3 Results and Discussion

The geometry of the investigated 3D MOSFET is given in Fig. 1: an n-channel MOSFET with an $1\mu m$ x $1\mu m$ channel and gate oxide of $15nm$. For demonstrating the influence of the oxide-body we selected two different shapes for the interfaces. Fig. 3 and Fig. 4 illustrate the potential distribution in channel length and width direction at the gate oxide semiconductor interface for nonrectangular and rectangular shape of the field oxide interface, respectively. These plots show how the potential distribution will be influenced by using rectangular shapes for the oxide body instead of the more realistic models as shown by Fig. 2. The high increase of the potential distribution out of the channel is due to the gate contact overlapping the field oxide. In the same way the carrier distribution is changed. A high gradient in the field oxide shape results in high parasitic current at the channel edge on the other hand this effect is less significant for low gradients.

## Acknowledgement

This work was supported by the research laboratories of SIEMENS AG at Munich, FRG, by DIGITAL EQUIPMENT CORP. at Hudson, USA, and by the "Fonds zur Förderung der wissenschaftlichen Forschung", project S43/10. We are indebted to Prof. H. Pötzl for many helpful discussions.

## References:

[1] S.M. Sze, Physics of semiconductor devices, ISBN 0-471-09837-X, John Wiley & sons, 1981

[2] S.M. Sze, VLSI-Technology, ISBN 0-07-062686-3, McGraw-Hill, 1983

[3] T. Iizuka,K.Y. Chiu, and J.L. Moll, Double threshold MOSFETs in

bird's–beak free structures, IEEE Int. Electron Device Meet.,Wash.,D.C., 1981, p. 380

[4] L.A. Hageman,Franklin T. Luk,David M. Young, On the equivalence of certain iterative acceleration methods, SIAM J.NUMER.ANAL., pp 852-873, vol. 17 No. 6, Dec 1980

[5] R.G. Grimes,D.R. Kincaid,D.M. Young, ITPACK 2A – A fortran implementation of adaptive accelerated iterative methods for solving large sparse linear systems, Report CNA-164, Center for numerical analysis, University of texas at Austin, 1980

[6] W. Hänsch, M. Miura–Mattausch, A new current relation for hot electron transport, Proc. NASECODE IV Conf.,pp.311-314, Boole Press, Dublin, 1985.

[7] S. Selberherr, Analysis and simulation of semiconductor devices , ISBN 3-211-81800-6, Springer, WIEN NEW-YORK, 1984

[8] O. Axelsson, Solution of linear systems of equations;Iterative methods, Lecture notes in mathematics 574, SMT, 1976

[9] S. Selberherr, The status of MINIMOS, Proc. Simulation of semiconductor devices and processes, pp 2-15, Swansea, 1986

[10] G.E. Forsythe,W.R. Wasaw, Finite Difference Methods for Partial Differential Equations. Wiley, NEW-YORK, 1960

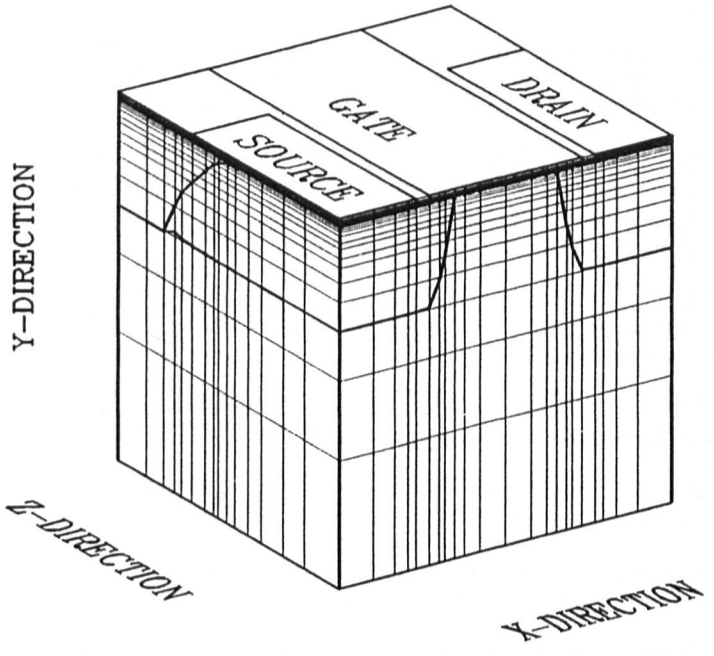


Fig.1: Perspective view of the three–dimensional MOSFET structure.

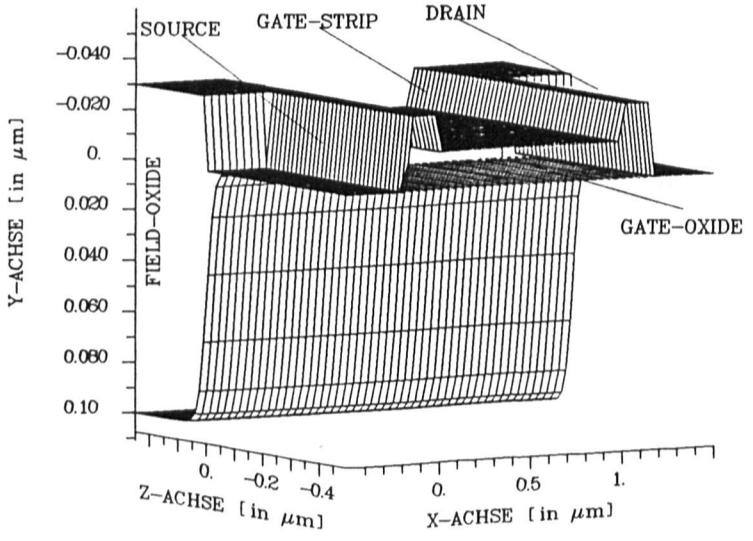


Fig.2: Oxide body of the MOSFET structure (the oxide is between the upper and lower plane).

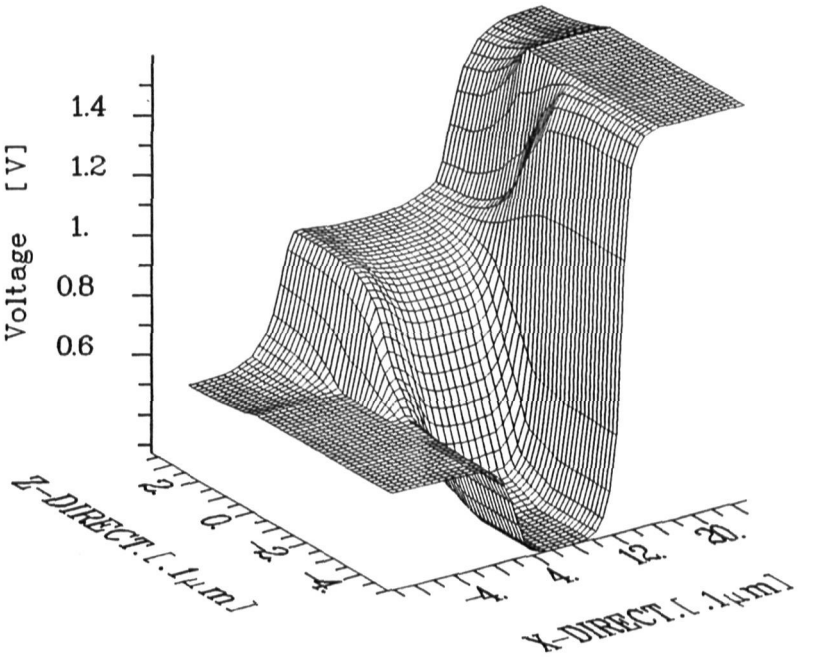


Fig.3: 3D–plot showing a detailed view of the surface potential at the channel edge along the channel length at bias $U_{DS} = 1.0V$, $U_{BS} = 0.0V$, $U_{GS} = .5V$ and a nonrectangular shape of the field–oxide.

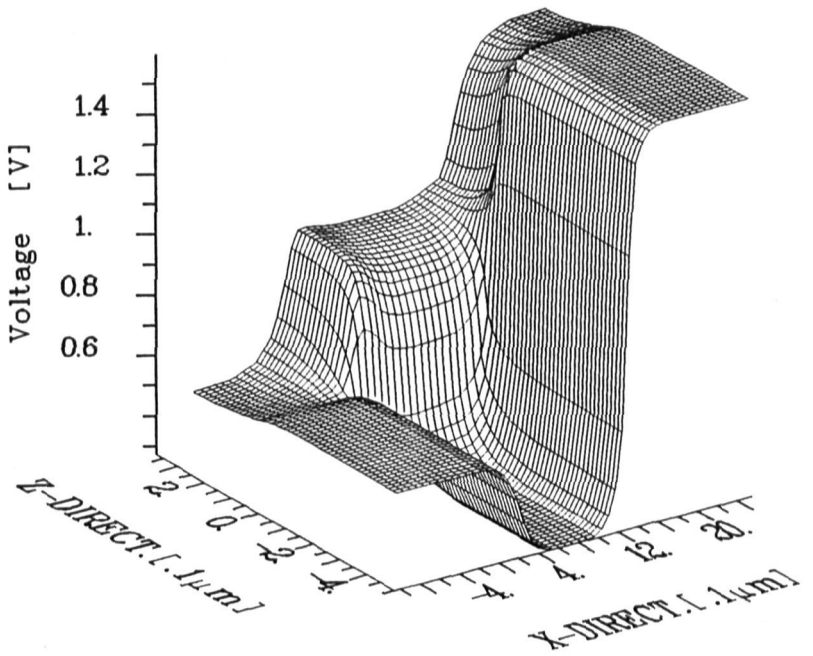


Fig.4: 3D–plot showing a detailed view of the surface potential at the channel edge along the channel length at bias $U_{DS} = 1.0V$, $U_{BS} = 0.0V$, $U_{GS} = .5V$ and a rectangular shape of the field–oxide.